

**Zeitschrift:** Helvetica Physica Acta

**Band:** 55 (1982)

**Heft:** 6

**Artikel:** Superconducting parameters of a strongly anisotropic intercalated TaS<sub>2</sub> compound : K<sub>0.33</sub>(H<sub>2</sub>O)<sub>0.66</sub>TaS<sub>2</sub>

**Autor:** Gygax, S. / Biberacher, W. / Lerf, A.

**DOI:** <https://doi.org/10.5169/seals-115311>

### **Nutzungsbedingungen**

Die ETH-Bibliothek ist die Anbieterin der digitalisierten Zeitschriften. Sie besitzt keine Urheberrechte an den Zeitschriften und ist nicht verantwortlich für deren Inhalte. Die Rechte liegen in der Regel bei den Herausgebern beziehungsweise den externen Rechteinhabern. [Siehe Rechtliche Hinweise.](#)

### **Conditions d'utilisation**

L'ETH Library est le fournisseur des revues numérisées. Elle ne détient aucun droit d'auteur sur les revues et n'est pas responsable de leur contenu. En règle générale, les droits sont détenus par les éditeurs ou les détenteurs de droits externes. [Voir Informations légales.](#)

### **Terms of use**

The ETH Library is the provider of the digitised journals. It does not own any copyrights to the journals and is not responsible for their content. The rights usually lie with the publishers or the external rights holders. [See Legal notice.](#)

**Download PDF:** 02.04.2025

**ETH-Bibliothek Zürich, E-Periodica, <https://www.e-periodica.ch>**

# Superconducting parameters of a strongly anisotropic intercalated TaS<sub>2</sub> compound: K<sub>0.33</sub>(H<sub>2</sub>O)<sub>0.66</sub>TaS<sub>2</sub>

By S. Gygax,<sup>\*)</sup> W. Biberacher and A. Lerf, Walther Meissner  
Institut für Tieftemperaturforschung der Bayerischen Akademie  
der Wissenschaften, D-8046 Garching

M. Denhoff, Simon Fraser University, Burnaby, British Colum-  
bia, Canada V5A 1S6

(1. II. 1983)

*Abstract.* Electrochemically intercalated K<sub>0.33</sub>(H<sub>2</sub>O)<sub>0.66</sub>TaS<sub>2</sub> crystals show a strong temperature dependent anisotropy of  $H_{c2}$  rising from 33 near  $T_c$  to well over 60 at lower temperatures. The coherence distances are determined to be  $\xi_{\parallel}(0) = 2.95 \times 10^{-6}$  cm and  $\xi_{\perp}(0) = 9.0 \times 10^{-8}$  cm. Penetration depths were estimated from low field measurements to be  $\lambda_{\parallel}(0) = 3.4 \times 10^{-4}$  cm and  $\lambda_{\perp}(0) = 7.1 \times 10^{-3}$  cm. An anomaly in the angular dependence of the entrance field  $H_{en}$  and trapped flux near parallel applied fields is found, qualitatively similar to what was observed in NbSe<sub>2</sub>.

## 1. Introduction, sample preparation

A recent study by Biberacher et al. [1] on electrointercalation of 2H-TaS<sub>2</sub> single crystals has shown that K<sub>x</sub>(H<sub>2</sub>O)<sub>y</sub>TaS<sub>2</sub> compounds can be prepared which have very sharp superconducting transitions. The highest  $T_c$  (5.6 K) is obtained for K<sub>0.33</sub>(H<sub>2</sub>O)<sub>0.66</sub>TaS<sub>2</sub> and initial measurements revealed a high  $dH_{c2\parallel}/dT$  and a large anisotropy in  $H_{c2}$ . This study reports on  $H_{c2}$  measurements on such crystals up to 7.5 T and on low field magnetic transitions. The measurements were used to determine coherence distance and penetration depth. We also investigated a curious angular dependence of the entrance field and trapped flux for near parallel directions with respect to the crystal planes. Such an effect, thought to be connected with the anisotropy, was previously observed on NbSe<sub>2</sub> [2].

The starting material for these compounds were 2H-TaS<sub>2</sub> crystals which were grown by the vapour transport method as 1T material and then subsequently annealed to form the 2H polymorph. The compounds were formed by electrochemical intercalation of individual crystals from an aqueous K<sub>2</sub>SO<sub>4</sub> solution. Details of this preparation method and the resulting charge transfer have been given earlier [1]. The samples were measured immediately after preparation except for the low field data which had to be taken in an other laboratory (see section 4).

<sup>\*)</sup> On leave from Simon Fraser University, Burnaby, British Columbia, Canada V5A 1S6

## 2. $H_{c2}$ measurements, coherence distances

$H_{c2}$  was obtained by an ac method where the sample was placed in a coil of a tank circuit whose frequency change was measured. The sample in its tank-coil assembly could be rotated in the field of a superconducting solenoid. The sample was heated through its superconducting transition in a fixed field. The low-field transitions were quite sharp (transition widths  $\sim 0.1$  K). We label as  $T(H_{c2})$  the temperature at which the linear transition region crosses the normal state value (see Fig. 1). Figure 2 shows the temperature dependences of  $H_{c2\parallel}$  and  $H_{c2\perp}$ .  $H_{c2\parallel}$  shows a tail near  $T_c$  and  $H_{c2\perp}$  has upward curvature through the whole temperature range. The tail in  $H_{c2\parallel}$  seems to be a common feature of intercalated layer compounds and could be due to a spread in  $T_c$  in these materials. Figure 3 is a plot of the anisotropy  $\varepsilon = H_{c2\parallel}/H_{c2\perp}$  in the upper critical field as a function of temperature. It shows a rapidly increasing anisotropy to values well above 60.

The  $H_{c2}$  measurements can be used to determine coherence lengths  $\xi_{\parallel}(0)$  and  $\xi_{\perp}(0)$  through the relations

$$\xi_{\parallel}^2(0) = \frac{\phi_0}{2\pi T_c (dH_{c2\perp}/dT)_{T_c}} \quad (1a)$$

$$\xi_{\perp}(0) = \frac{\phi_0}{2\pi T_c \xi_{\parallel}(0) (dH_{c2\parallel}/dT)_{T_c}} \quad (1b)$$

One finds  $\xi_{\parallel}(0) = 2.95 \times 10^{-6}$  cm and  $\xi_{\perp}(0) = 9.0 \times 10^{-8}$  cm, where the latter value was obtained using the slope of  $H_{c2\parallel}$  at 5.5 K, slightly below  $T_c$ .

## 3. Dimensional crossover

The  $H_{c2}$  data should be compared with the theory developed for such layer compounds by Klemm, Luther and Beasley (KLB) [3]. The important parameters

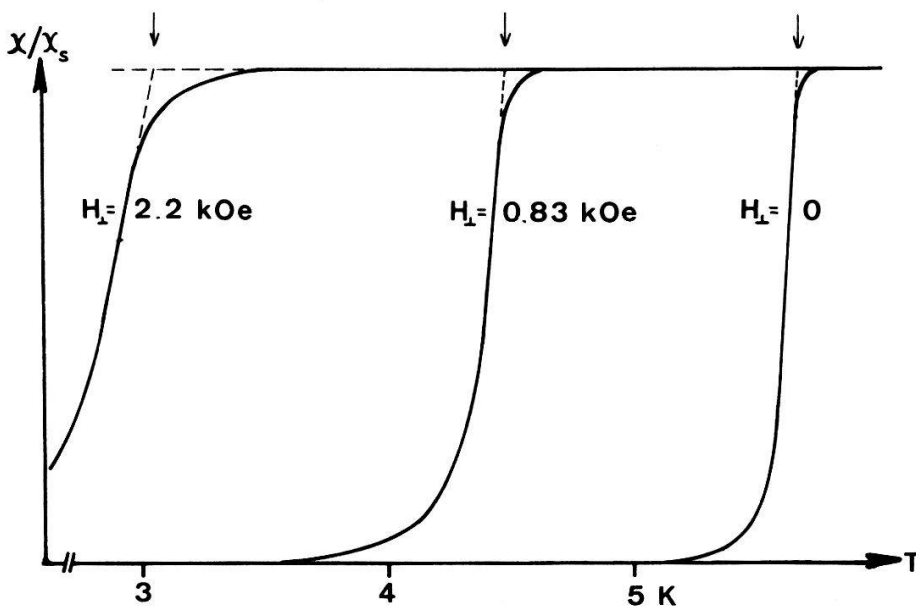


Figure 1

ac transition in constant field for the perpendicular direction. The arrows indicate our choice for  $T(H_{c2})$ .

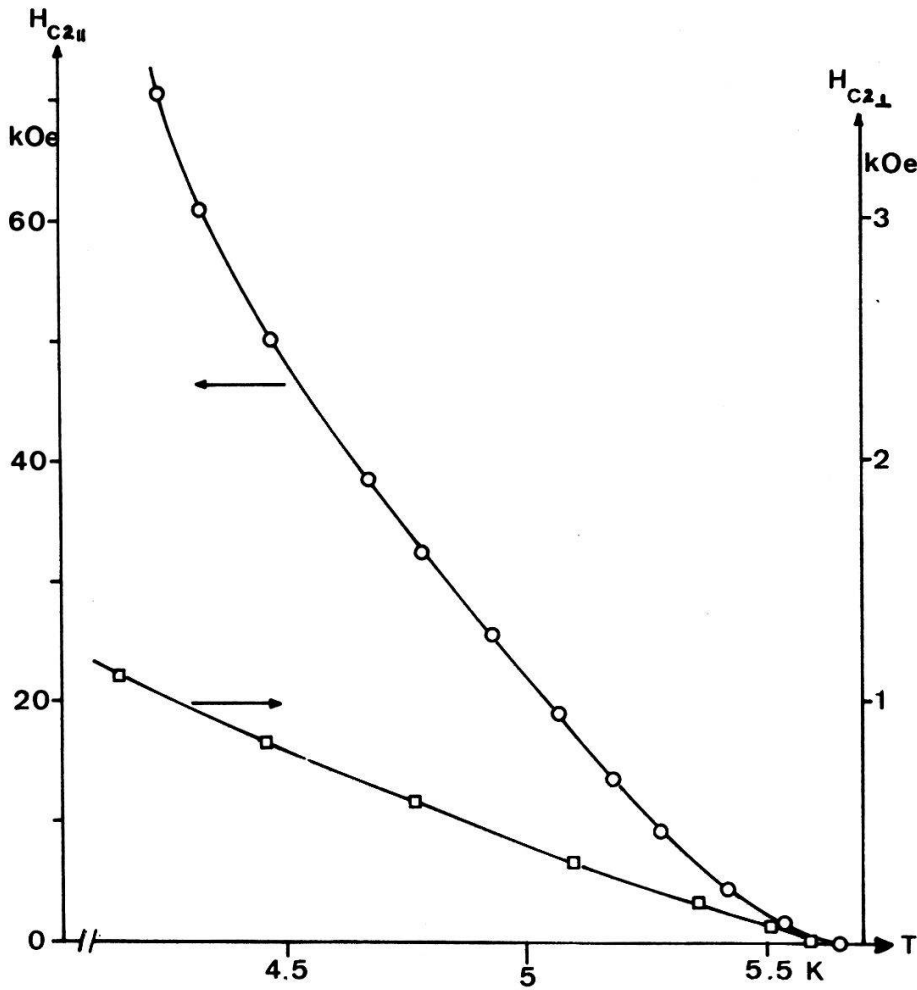


Figure 2

The critical fields  $H_{c2||}$  and  $H_{c2\perp}$  as a function of temperature.

are

$$r = \frac{4}{\pi} \left( \frac{\xi_{\perp}(0)}{s/2} \right)^2 \quad (2)$$

which describes the decoupling of the layers,  $s$  being the interlayer distance, and

$$\alpha = \frac{(dH_{c2||}/dT)_{T_c}}{4k_B T_c / \pi \mu_B} \quad (3)$$

which indicates the importance of paramagnetic limiting. The third parameter in the theory, the spin-orbit scattering time  $\tau_{so}$  has to be regarded as a fitting parameter since it is at present not directly accessible by experiment. From our experiments we find  $r = 5.1$ , and  $\alpha = 1.7$  (again ignoring the tail). A complete fit of our  $H_{c2}$  data to the KLB theory would be desirable. However our available field does not allow  $H_{c2||}$  to be followed to low enough temperatures to extract meaningful parameters. Nevertheless the experimentally determined value of  $r = 5.1$  and the strong temperature dependence of the anisotropy  $\epsilon(T)$  suggest that dimensional crossover is likely.

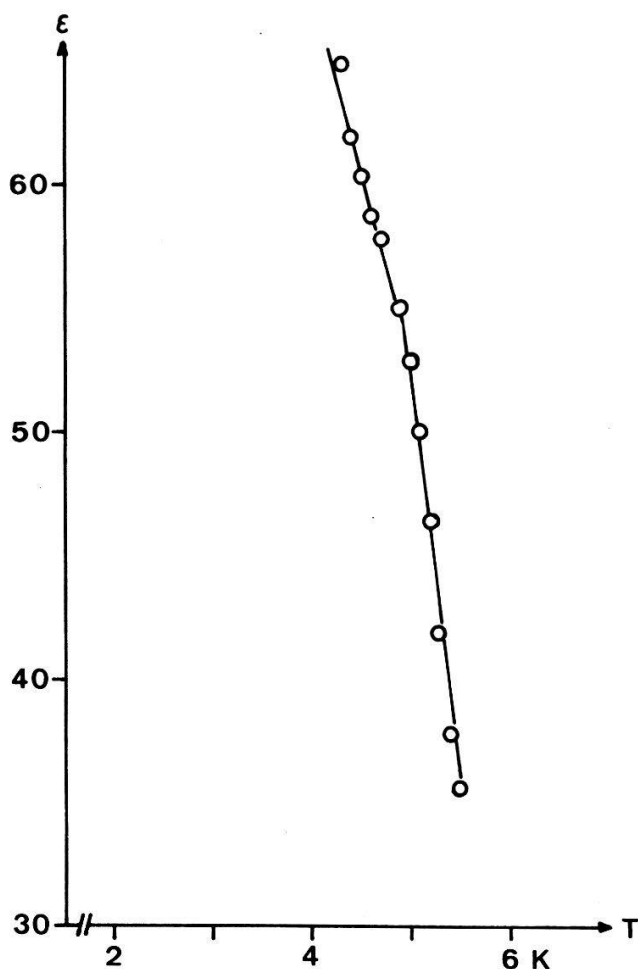


Figure 3

Anisotropy  $\varepsilon = H_{c2\parallel}/H_{c2\perp}$  as a function of temperature.

#### 4. Low-field data

One of our samples was placed in a saturated aqueous solution of  $K_2SO_4$ , flown from Munich to Vancouver, placed in a refrigerator for 2 weeks and then investigated in low fields in a SQUID magnetometer. Transition curves in constant fields were taken and analyzed as described earlier [2]. An additional feature was a second set of field coils which produces a field perpendicular to the longitudinal field. This allowed a rotation of the total field away from the axial symmetry of the pick-up loop. Magnetization measurements on a small Pb cylinder mounted at  $45^\circ$  with respect to the axial symmetry direction provided the calibration of the magnetic tilt angle. The angle  $\theta_a$  between the applied field and the  $c$ -axis (perpendicular to the layers) of the sample could then be changed easily while keeping the sample in the pick-up loop fixed.

##### 4.1. Entrance field, trapped flux

The magnetization curves permit a determination of  $H_{en}(T)$ , the applied field at which flux first enters the sample. We expect  $H_{en}$  to be larger than  $H_{c1}$  due to

pinning. We observe a linear  $H_{en}(T)$  dependence near  $T_c$ . The angular dependence of  $dH_{en}/dT$  near  $\theta_a = 90^\circ$  is plotted in Fig. 4. It shows pronounced structure, symmetric around  $90^\circ$ . In fact this symmetry was used to determine the  $\theta_a = 90^\circ$  angle (the error in the alignment amounted to  $\sim 0.5^\circ$ ). The observed structure is of the same form as the one found in our measurements of  $H_{en}(\theta_a)$  in NbSe<sub>2</sub>. The entrance field, instead of increasing with increasing angle suddenly breaks away to lower values and decreases to the  $H_{en}(90)$  value. In NbSe<sub>2</sub> this break was sample dependent because of demagnetization effects. We argued that it was caused by preferential alignment of the flux lines either parallel or perpendicular to the crystal planes. This critical angle of the applied field  $\theta_{ac}$  at which the fluxline-flip should occur is given by

$$\theta_{ac} = \arctg [H_{en}(90)/H_{en}(0)] \quad (4)$$

Using the measured values of  $dH_{en}/dT$  both perpendicular ( $0^\circ$ ) and parallel ( $90^\circ$ ) to the layers, we had found very good agreement between this simple model and the observed position of the break for all sample shapes studied. Also found was a corresponding structure at the same angle in the amount of trapped flux. Although the structure of  $H_{en}$  in the  $K_{0.33}(H_2O)_{0.66}TaS_2$  sample has the same general shape as in NbSe<sub>2</sub>, the location of the break does not agree with  $\theta_{ac}$  calculated from equation (4). The measured values of  $dH_{en}(90)/dT = 12.2$  Oe/K and  $dH_{en}(0)/dT = 6.6$  Oe/K give  $\theta_{ac} = 61.6^\circ$  while the maximum in  $dH_{en}(\theta_a)/dT$  occurs at  $87^\circ$ . We did in one run observe some structure around  $60^\circ$  but the pronounced break at  $87^\circ$  was also present. We also measured the trapped flux relative to the full transition signal by subsequently cooling the sample in the same applied field. (Removing the field and warming once more did not change the amount of trapped flux.) As in NbSe<sub>2</sub> there is a close relationship between the angular dependencies of the trapped flux (Fig. 5) and  $H_{en}$  (Fig. 4). Both show the same pronounced structure at the same angle  $\theta_a = 87^\circ$ . This would indicate that there is a much closer relationship between pinning and fluxline alignment than we previously thought. This seems to become more pronounced in crystals with

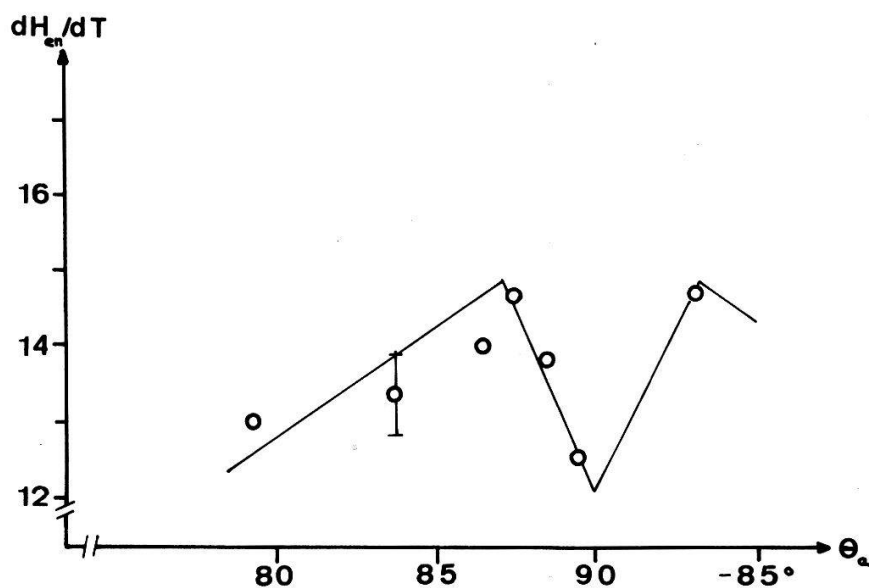


Figure 4  
Angular dependence of the entrance field  $H_{en}$  near the parallel direction.

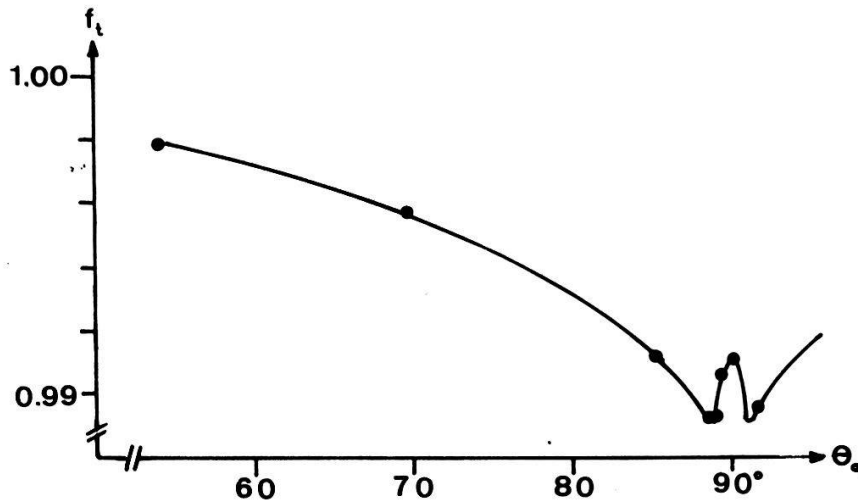


Figure 5

Angular dependence of the trapped flux.

very high anisotropy. It also indicates that crystal alignment for parallel fields becomes very important. This was observed in our  $H_{c2}$  measurements as well. The ac transition curves in high fields show very pronounced structure due to flux jumps for a narrow angular range ( $\sim 1^\circ$ ) around parallel alignment.

#### 4.2. Penetration depth

The low field transition curves have a long tail below  $T_c$ . This should make it possible to estimate the penetration depth. We use the following notation. In the case of coherence distances  $\xi_{\parallel}$  stands for the characteristic length scale over which order parameter changes occur within the layer planes. We similarly take  $\lambda_{\parallel}$  to mean the characteristic length scale over which current distributions shield out a field perpendicular to the layers. These shielding currents flow parallel to the planes which is reflected in the notation.

(a) Field perpendicular to the planes ( $\theta_a = 0^\circ$ )

We approximate the crystal by an oblate spheroid of diameter  $2r'(T) = 2(r - \lambda_{\parallel}(T))$  and height  $2t$ . Since these dimensions are small compared to the astatic pick-up loop radius  $R$  we can use the dipole approximation for the calculation of the resulting flux due to the diamagnetic ( $\chi = -1/4\pi$ ) sample [4],

$$\phi = p \frac{2\pi}{R} = \frac{4\pi}{3} r'^2 t H_a [4\pi(1 - N/4\pi)]^{-1} \frac{2\pi}{R}$$

Since  $r'/t \gg 1$  we can express the demagnetization term:

$$[4\pi(1 - N/4\pi)]^{-1} \approx \frac{r'}{2\pi^2 t}$$

We then have:

$$\phi(T) = \frac{4[r - \lambda_{\parallel}(T)]^3}{3R} H_a$$

and

$$\frac{\phi(T)}{\phi(0)} = \frac{(r - \lambda_{\parallel})^3}{[r - \lambda_{\parallel}(0)]^3}$$

or

$$\left[ \frac{\phi(T)}{\phi(0)} \right]^{1/3} = \frac{1}{1 - \lambda_{\parallel}(0)/r} - \frac{\lambda_{\parallel}(0)/r}{1 - \lambda_{\parallel}(0)/r} Z(T) \quad (5)$$

For our estimate of  $\lambda$  we will use the Gorter–Casimir temperature dependence:  $Z(T) = [1 - (T/T_c)^4]^{-1/2}$  and determine  $\lambda_{\parallel}(0)$  from a least-square fit to the data. Since the sample has non-circular crosssection we measure the circumference  $C$  and determine an average  $r$  through  $r = C/2\pi$ .

(b) Field parallel to the planes ( $\theta_a = 90^\circ$ )

We now approximate the crystal by a plate of width  $2r$  and thickness  $2t$ . Figure 6 shows the geometry and identifies  $\lambda_{\parallel}$  and  $\lambda_{\perp}$ . Since we now have negligible demagnetization factors we write

$$\begin{aligned} \frac{\phi(0) - \phi(T)}{\phi(0)} &\approx \frac{\lambda_{\perp} - \lambda_{\perp}(0)}{r} + \frac{\lambda_{\parallel} - \lambda_{\parallel}(0)}{t} \\ &= (Z - 1) \left[ \frac{\lambda_{\perp}(0)}{r} + \frac{\lambda_{\parallel}(0)}{t} \right] \end{aligned} \quad (6)$$

again using the Gorter–Casimir temperature dependence.

(c) Results

The procedure outlined above gives the following estimates for the penetration depths:

$$\lambda_{\parallel}(0) = 3.4 \times 10^{-4} \text{ cm} \quad \text{and} \quad \lambda_{\perp}(0) = 7.1 \times 10^{-3} \text{ cm}$$

But unlike the  $H_{c2}$  measurements which were done immediately after the electrochemical intercalation these measurements were done on a sample which was kept for a prolonged period in a supersaturated solution at room temperature. Its  $T_c$  was substantially lower (4.45 K) than what is measured on a fresh sample (5.6 K), indicating a decreased charge transfer. In one run the  $T_c$  had decreased to

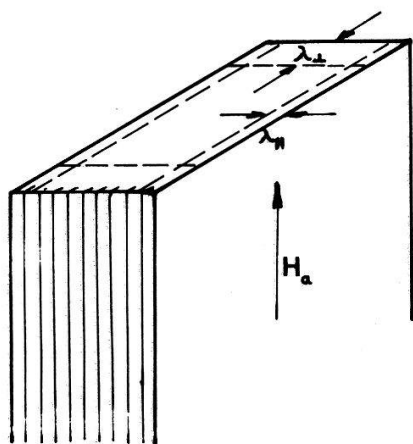


Figure 6

Schematic drawing of a layered crystal in parallel applied field showing penetration depths.



4.0 K but the values of the penetration depths remained unchanged. A similar effect is observed for the slopes of  $H_{c2}$ . A sample which had a  $T_c$  of 5.2 K still had the same initial slope for  $H_{c2}$  parallel and perpendicular as the ones with a  $T_c$  value of 5.6 K. This would indicate that the above estimates of  $\lambda$  are not too far from the values one would obtain in a fresh sample. Simultaneous measurements of high and low field transition curves are clearly needed.

In addition the approximations which are implicit in equations 5 and 6 have to be modified since the sample dimensions are not very much larger than the penetration depths.

## 5. Anisotropy

The strong temperature dependence of the anisotropy in  $H_{c2}$  shown in Fig. 3 is a feature of weakly coupled layered compounds. It was observed also for intercalations of TaS<sub>2</sub> with aniline [5], methylamine and dimethylamine [6]. It is a consequence of the rapidly increasing  $H_{c2\parallel}$  when  $\xi(T)$  reaches the same order as the layer separation. In the KBL theory the temperature dependence of  $\epsilon$  becomes stronger the smaller the parameter  $r$  of equation 2. The experimentally determined value of  $r = 5.1$  seems somewhat large but it may indicate that the interlayer coupling is not only a function of the geometrical layer separation  $s$  but may also depend on the tunnelling probability.

The coherence distances were calculated from  $H_{c2}$  measurements near  $T_c$  where the Ginzburg–Landau equations with an anisotropic mass should be valid. Implicit in the expression for  $\xi(0)$  in equation 1 are a linear temperature dependence for  $H_{c2}$  and the Ginzburg–Landau temperature dependence for  $\xi$ :

$$\xi(T) = \xi(0)(1 - T/T_c)^{-1/2} \quad (7)$$

We then find for the anisotropy in the coherence distances  $\xi_{\parallel}(0)/\xi_{\perp}(0) = 33$  which corresponds to the anisotropy of  $H_{c2}$  near  $T_c$ . Using the Ginzburg–Landau expression of equation 7 makes the anisotropy of  $\xi$  temperature independent in contrast to the strong temperature dependence of the  $H_{c2}$  anisotropy. An alternate approach [6] fixes the temperature dependences of  $\xi$  not by equation 7 but through the relations

$$\xi_{\parallel}(T) = \left[ \frac{\phi_0}{2\pi H_{c2}(T)} \right]^{1/2} \quad (8a)$$

$$\xi_{\perp}(T) = \frac{\phi_0}{2\pi \xi_{\parallel}(T) H_{c2\parallel}(T)} \quad (8b)$$

Experimentally equation (8a) turns out to be indistinguishable from equation 7 and gives the same  $\xi_{\parallel}(0)$  as quoted in Section 2. Equation (8b) however results in a much faster drop of  $\xi_{\perp}(T)$  with temperature than given by equation 7 due to the strong increase in  $H_{c2\parallel}$ . Also  $r$  becomes smaller. But the anisotropy is now the same as the anisotropy of  $H_{c2\parallel}$  and therefore strongly temperature dependent. Further work is required to determine which of the two approaches is appropriate for strongly anisotropic superconductors.

The analysis in Section 4.2 leading to estimate of the penetration depths  $\lambda$

made use of the Gortner–Casimir temperature dependence in both principal directions. This automatically gives a temperature independent anisotropy of  $\lambda$ :  $\lambda_{\perp}(0)/\lambda_{\parallel}(0) = 21$ . This anisotropy is smaller than both the anisotropy of  $\xi$  and  $H_{c2}$  near  $T_c$ . We have already pointed out the problem with sample deterioration and the number of approximations necessary to obtain these values. But in the case of the penetration depths it should in principle be possible to determine the actual temperature dependences for both directions if proper sample geometries are chosen.

One of us (S.G.) would like to thank Prof. K. Andres and the WMTTF for the kind hospitality.

#### LITERATURE

- [1] W. BIBERACHER, A. LERF, J. O. BESENHARD, H. MÖHWALD, T. BUTZ and S. SAIBENE, to appear in *Nuovo Cimento*.
- [2] M. W. DENHOFF and S. GYGAX, *Phys. Rev. B* 25, 4479 (1982).
- [3] R. A. KLEMM, A. LUTHER and M. R. BEASLEY, *Phys. Rev. B* 12, 877 (1975).
- [4] M. W. DENHOFF, S. GYGAX and J. R. LONG, *Cryogenics* 21, 400 (1981).
- [5] D. E. PROBER, M. R. BEASLEY and R. E. SCHWALL, *Phys. Rev. B* 15, 5245 (1977); D. E. PROBER, R. E. SCHWALL and M. R. BEASLEY, *Phys. Rev. B* 21, 2717 (1980).
- [6] J. L. VICENT, S. J. HILLENUS and R. V. COLEMAN, *Phys. Rev. Lett.* 44, 892 (1980).

